Mechanical behavior and fracture characteristics of polymeric pipes under curved three point bending tests: Experimental and numerical approaches

Houcine Jemii, Amir Bahri, Rym Taktak, Noamen Guermazi, Frédéric Lebon

Mechanical behavior and fracture characteristics of polymeric pipes under curved three point bending tests: Experimental and numerical approaches

Houcine Jemii [a, *], Amir Bahri [a], Rym Taktak [b], Noamen Guermazi [a], Frédéric Lebon [c]

[a] Laboratoire de Génie des Matériaux et Environnement (LGME), Ecole Nationale d'Ingénieurs de Sfax (ENIS), Université de Sfax, BP 1173-3038. Sfax, Tunisia
[b] Laboratoire des Matériaux Avancés (LMA), Ecole Nationale d'Ingénieurs de Sfax (ENIS), BP 1173-3038. Sfax, Tunisie Université de Sfax, Tunisia
[c] Aix Marseille Univ, CNRS, Centrale Marseille, LMA UMR 7031, 4 impasse Nikola Tesla, F-13013 Marseille, France

This study describes an investigation of the load–deflection response of the material used for production of polymeric pipes. Three point bending tests were performed on curved pipe samples to evaluate their flexural properties, namely the flexural strength, the modulus, the strain to failure and the mode of failure. Effects of various configurations and parameters are investigated: effect of internal or external loading, effect of notch, impact of aging, combined effect of notch and aging. In addition, FE models are established to predict pipe material response under flexural loading. From the main results, the average flexural stress–strain response of pipe material is characterized by a linear portion curve, followed by a non-linear deformation up to the ultimate failure stress. A ductile behavior was observed, but with a brutal rupture at the peak flexural stress. The flexure behavior of the pipe material depends also on the configuration, and it behaves differently under internal and external loading. The presence of notch in pipe material reduces its mechanical performance. A significant decrease of flexural properties was observed for hydrothermal aged pipe samples. The combined effect of both hydrothermal aging and notch affects dramatically the flexural performance of pipe material. Consequently, the service life of pipe structures risks to be reduced. Finally, a coupled experimental–numerical approach for the characterization of pipe material behavior under flexure loading has shown a good correlation, and therefore, the efficiency of the established FE model to predict the flexural response of pipe structures.

1. Introduction

It is well known that polymers and polymer composite pipes have been widely used in various fields, namely, for evacuation of drinking water, water boreholes, petroleum and gas transportation because of their low cost of installation & maintenance and equally for their physico-chemical and mechanical properties [1–3].

Among thermoplastic materials, polyvinyl chloride (PVC) pipes are equally used for drinking and wastewater evacuation, window profiles, wire and cable insulation and medical devices [4,5,7], thanks to their mechanical and tribological properties [6–10]. PVC

* Corresponding author.
E-mail address: houcine@webmails.com (H. Jemii).

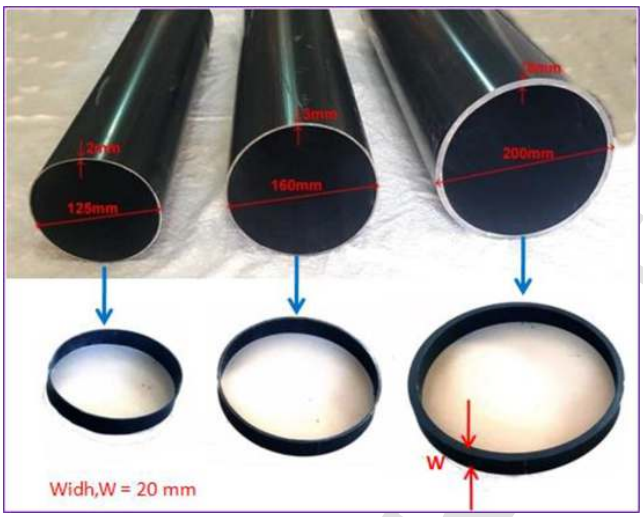

Fig. 1. Dimensions of polymeric pipes and extraction of samples for characterizations.

Fig. 2. Extraction and dimensions of curved samples dedicated for curved three point bending (CTPB) tests.

Table 1
The experimental program of the different flexural experiments.

Geometry	Temperature (°C)	Crosshead rate (mm/min)	Thickness h (mm)	Width W (mm)	*(a/h)* value
C-Shaped	23	0.5–5–50–250–500	8	20	0.5
	23	5	2–3–8	20	0.5
	23	5	8	20	0.5
	23	5	8	20	0.125–0.25–0.375–0.5
	25–60–90	5	8	20	0.5

pipes are characterized by high resistance to the impact, chemicals and corrosive environments [11–14]. Meanwhile, their mechanical properties can change with time and high constraint. When it is used in petroleum and water application, PVC pipes are subjected to high pressure resulting tensile and flexion. High constraint caused by flexion can affect their performances and lead to the failure and damage.

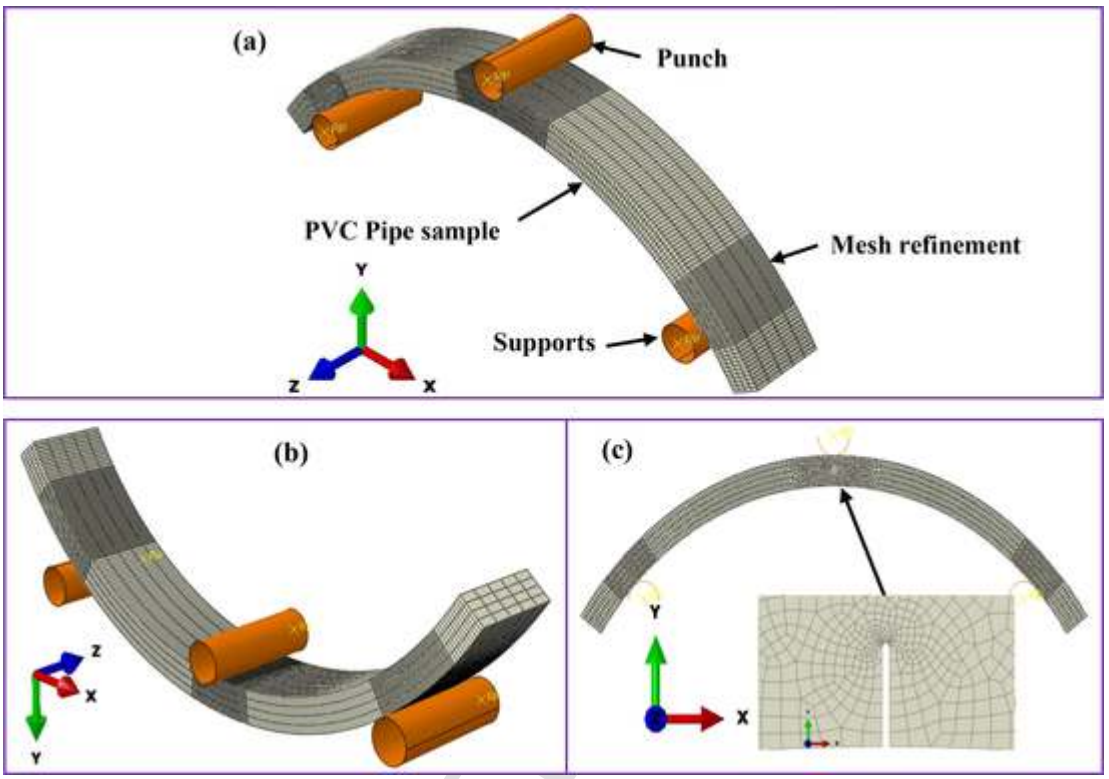

Fig. 3. Boundary conditions and mesh configuration of the three-point bending test: a) concave side down, b) concave side up, and c) Notched 2D model.

Table 2
XFEM parameters.

Ratio, a/h	Max principal stress Maxps (MPa)	Fracture energy, GF (J/m^2)
0.125	32	7.61
0.25		7.5
0.375		7.04
0.5		6.07

Recently, Al-Abtah et al., [15] have reported that, in service, pipes can be subjected to bending loading (called pipe bending), and consequently, compressive, tensile and also shear stresses can happen. Firouzsalari et al., [16] have focused on studying the energy absorption capacity for flax fabric-reinforced epoxy pipes subjected to lateral compression.

Babiak et al. [17] have considered that the appropriate way of assessing the effect of the mentioned stresses during bending is to use three or four-point bending tests.

Mandell et al., [18] have studied effects on the fracture toughness of rigid PVC pipes using flexural test. They have concluded that, over a range of temperatures and rates, the PVC pipe responses shift from ductile, notch-insensitive behavior to brittle.

In their work focusing on the brittle fracture process of PVC pipe material, McGarry et al. [4] have only considered brittle failures, despite that PVC pipe materials may fail in a ductile manner in service.

Aldea et al. [19] have used a specific flexural test for pipe (four-point loading apparatus) to characterize the flexural strength of pipe specimens. In such Ref, [19], the authors have considered the pipe as a beam working in flexure, and the calculations were carried out according to the elementary theory of beams.

On the other hand, many researchers have focused their attention to study the PVC mechanical properties under different mechanical loading tests following experimental and numerical approaches [11,14,20,21]. Experimental tests are usually needed to validate numerically-predicted results.

Jemii et al. [20] have studied the mechanical resistance of PVC pipes under a specific tensile test. They have designed and then developed split disk tensile (SDT) test in order to reproduce the internal pressure applied in the real industrial procedure. They have determined the circumferential mechanical characteristics and the mechanical strength of industrial PVC pipes.

In the present work, three point bending test has been conducted on the material used for production of pipes in order to analyze their performance when subjected to flexion test or external pressure. Various configurations and parameters are tested to enlarge the experimental study. One of the main objectives of this work is to assess flexure strength, material modulus, deformation and failure of

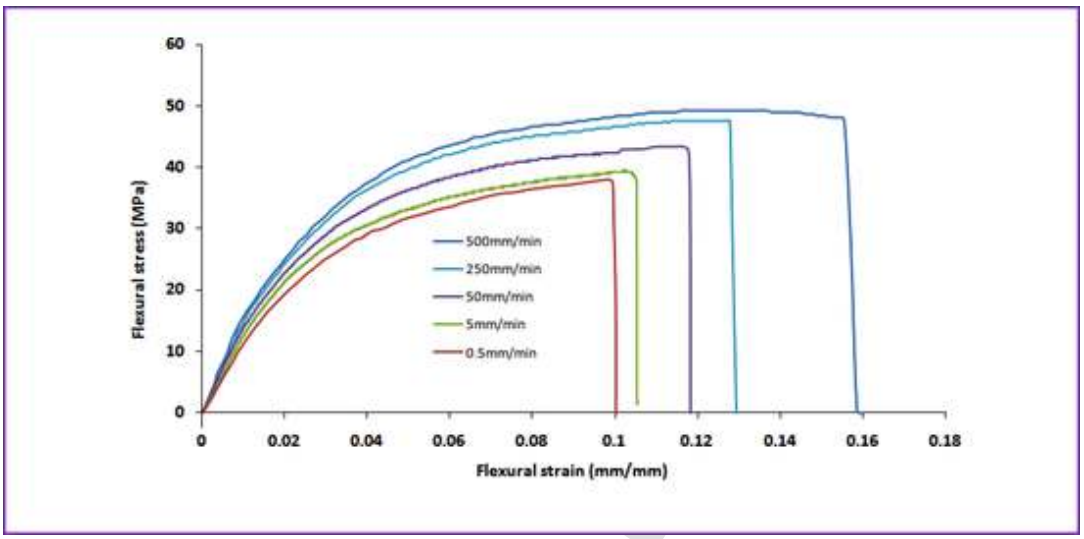

Fig. 4. Plot of flexural stress *vs.* flexural strain for pipe sample (with 8 mm of thickness) under various values of crosshead rates (0.5–500 mm/min).

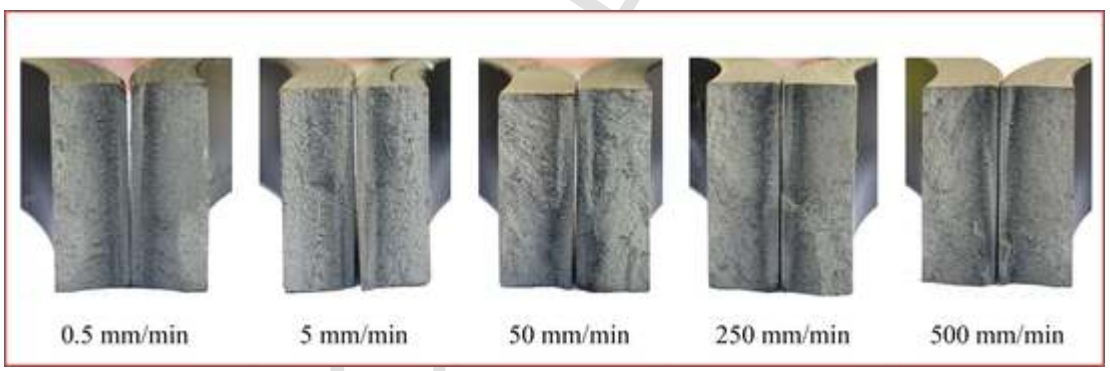

Fig. 5. Fractures surfaces of tested C-shaped PVC samples at crosshead rate from (0.5 to 500 mm/min).

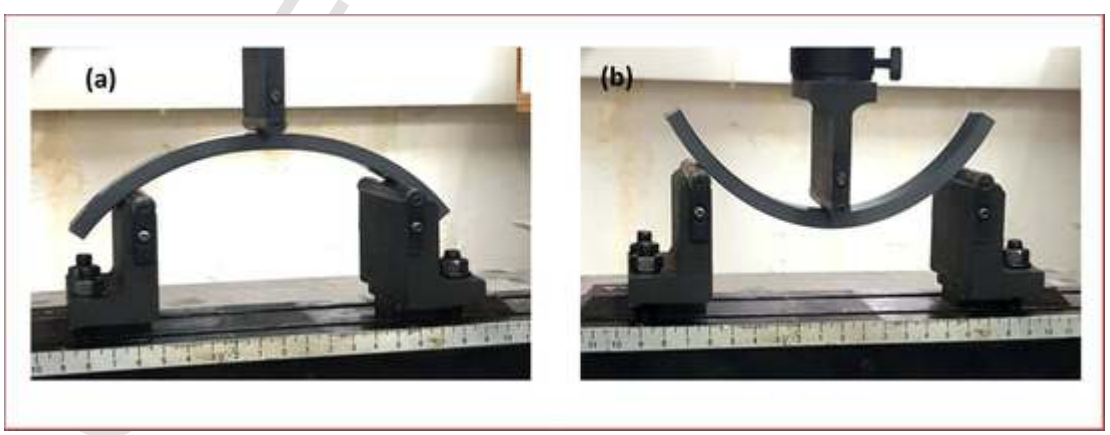

Fig. 6. Three point bending configurations applied on pipe curved samples: (a) Concave side down, (b) Concave side up.

pipe material under various configurations. Also, the new knowledge of this study is to consider the impact of the hygrothermal aging and the presence of artificial notch on the mechanical characteristics of material pipe. In addition, for some cases, FE models are established to predict pipe material under flexural loading. Then, experimental data and numerical results are evaluated and compared. The experimental/numerical correlation is then discussed to evaluate the robustness of the FE model.

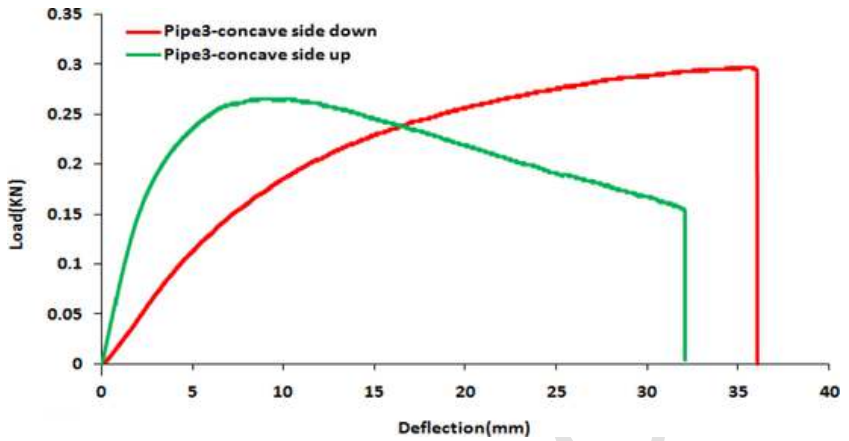

Fig. 7. Typical Load-Deflection curves of pipe material (thickness 8 mm) under various configurations: Concave side down; concave side up. (Value of crosshead speed 5 mm/min).

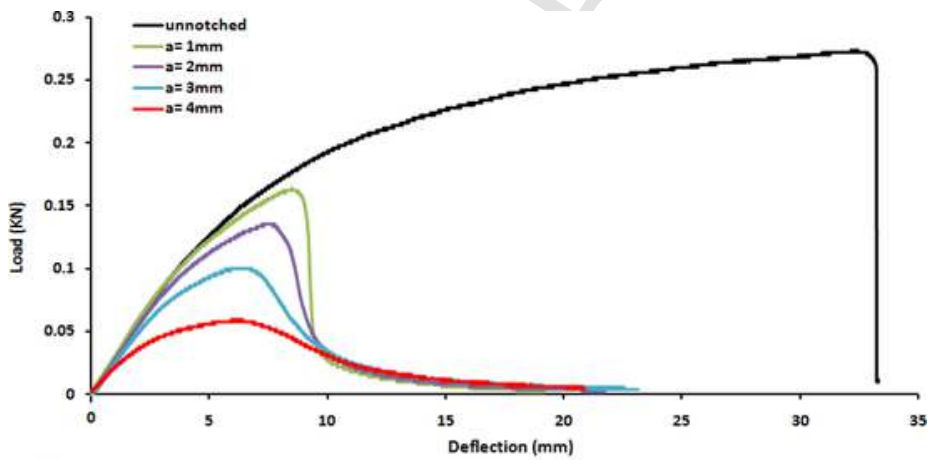

Fig. 8. Load-Deflection curves of pipe samples (8 mm thickness) without and with notch (different depths " a ") tested under a crosshead speed 5 mm/min.

2. Materials, techniques and methodology

2.1. Material and samples preparation

In this work, extruded polymeric pipes were supplied by Tuyauplast company, Gafsa, Tunisia. The pipes material is based on polyvinyl chloride (PVC) reinforced with calcium carbonate ($CaCO_3$) fillers, and mixed with a commercial dioctyl phthalate (DOP) as a plasticizer, as described elsewhere [22]. For tested samples, rings were cut transversely from extruded pipes, according to Fig. 1.

Moreover, from each sample illustrated in Fig. 1, three curved samples are cut to be tested in curved three point bending (CTPB) tests, as shown in Fig. 2. After that, the average value of the obtained results will be considered.

2.2. Experimental work and methodology

In this section, all flexure tests were conducted at room temperature on a WDW-10E universal test machine with 10 kN maximum load cell. At least three samples were tested for each test series and then the average curves were considered.

Here, it is also important to note that flexure experiments were performed on various conditions, namely, pipe samples with and without notch, samples with notch but with different depths, unaged and hydrothermally aged samples, different values of crosshead rate.

The experimental program that summarizes the different experiments with different parameters is given in Table 1.

For samples with initial notch, the tip of the notch was sharpened in mid-span with an electric jigsaw (2 mm thick) to a depth of a = 1, 2, 3 and 4 mm. This means *(a/h)*-ratio values of 0.125; 0.25; 0.375 and 0.5 of the sample thickness (h = 8 mm).

To examine the effect of aging on flexure properties, accelerated hydrothermal aging was considered. Pipe samples (Fig. 2) have been exposed to three temperatures (25, 60 and 90 °C) in distilled water for a period of 90 days.

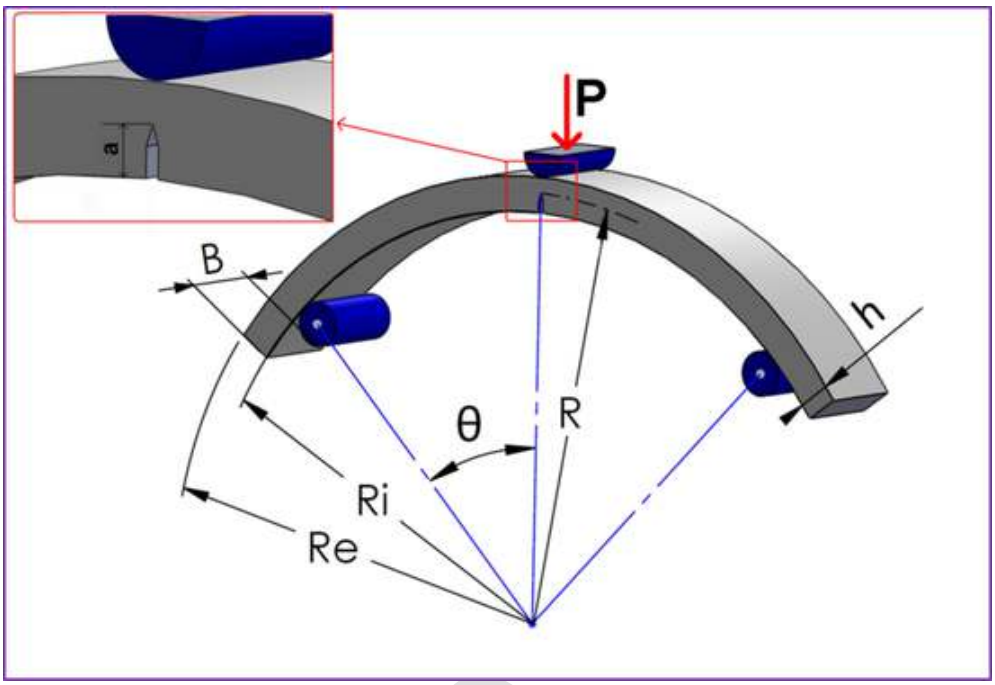

Fig. 9. Schematic illustration of C-shaped samples and the main dimensions used for K_I calculation.

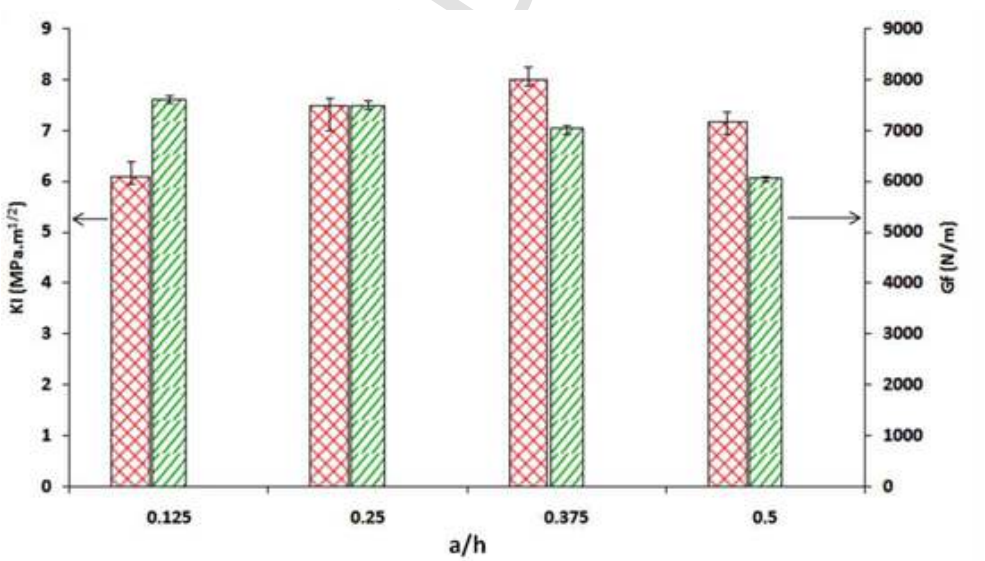

Fig. 10. Variation of stress intensity factors (KI) and Fracture energy versus the ratio (notch depth / sample thickness: a/h).

During the experiment, the curved sample is supported on two rollers and centrally loaded (under constant load) in a three-point bend configuration as shown in Fig. 2.

Finally, it is to note that for each flexure experiment, the obtained Load-Deflection curve was used to extract and estimate the flexural properties (the flexural strength (σ_f), the modulus (E_f) and the strain to failure (ε_f)).

The flexural moduli " E_f " were determined (from the slope "m" of initial linear portion of the Load-Deflection curve), according to Equation.1. The flexural strength and the flexure strain were calculated based on the following equations (Equation (2) and (3)), [21, 23]:

$$Ef = \frac{L^3 m}{4hW^3} \tag{1}$$

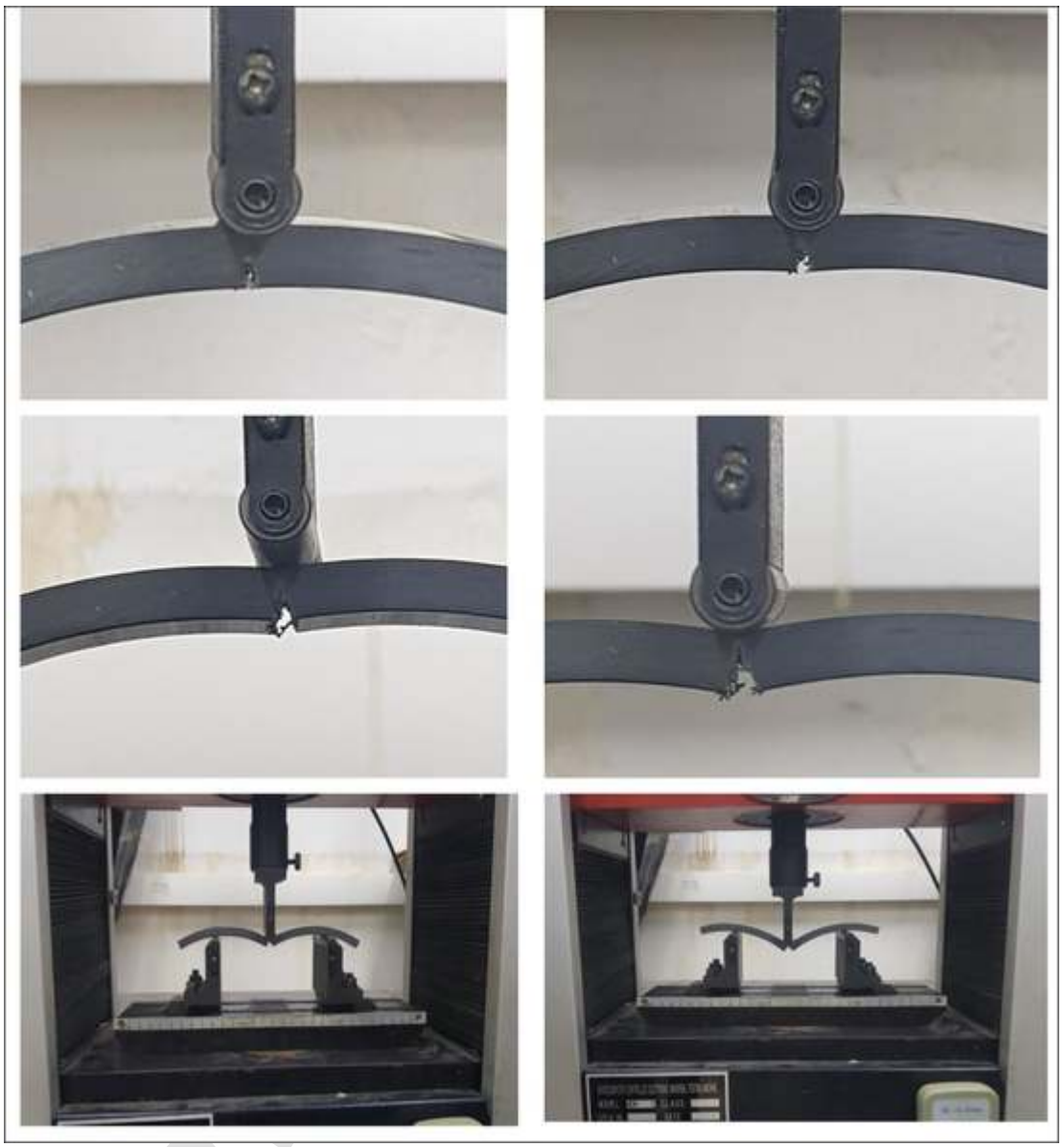

Fig. 11. Photo sequences on notch propagation during three point bending applied on notched-sample (h = 8 mm, a = 3 mm, crosshead speed = 5 mm/min).

$$\sigma f = \frac{3PL}{2BW^2} \quad \text{where } \frac{L}{h} \leq 16 \tag{2}$$

$$\varepsilon f = \frac{6DW}{L^2} \tag{3}$$

where P is the applied load, L is the support span, D is the maximum deflection of the center of the sample and h and W are the thickness and width of the sample beam.

2.3. Numerical modeling of curved three-point bending test

The numerical modeling of the three-point bending test has been built for three different configurations, namely, convex PVC bending test (model 1), convex PVC bending test coupled with a crack propagation (model 2) and concave bending test (model 3), Fig. 3. Numerical simulation test has been conducted using commercial nonlinear finite element (FE) code ABAQUS. Both dynamic explicit and static general calculation mode has been adopted during numerical simulation.

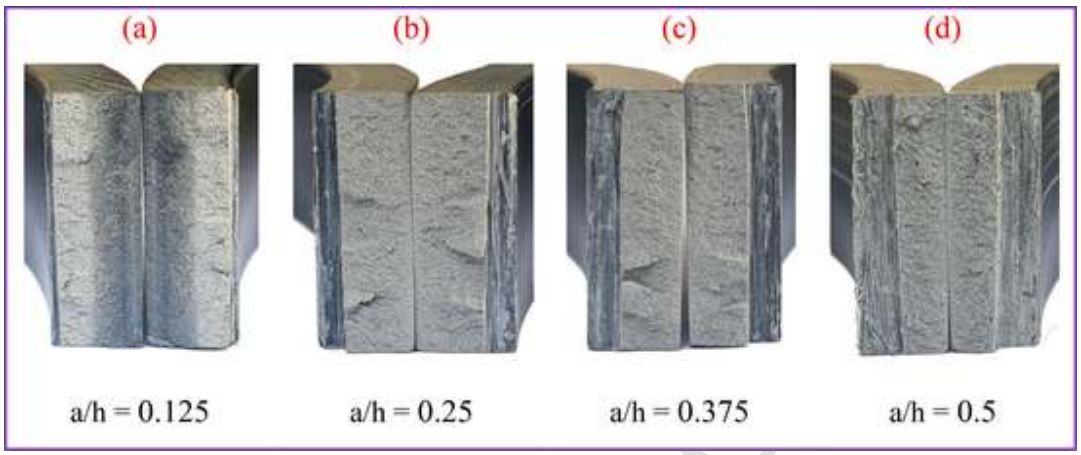

Fig. 12. Fractures surfaces of tested C-shaped notched PVC samples at crosshead rate of 5 mm/min.

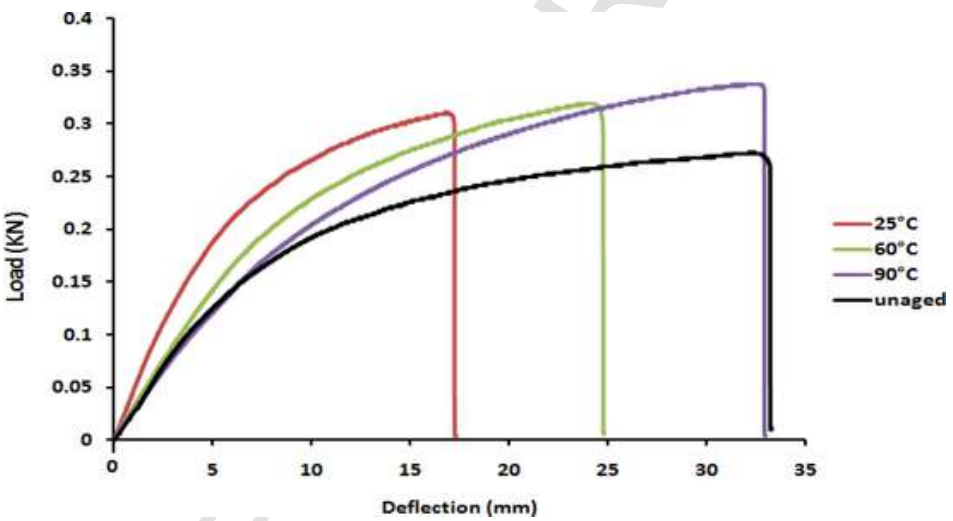

Fig. 13. Typical Load-Deflection curves of virgin and hydrothermally aged pipe samples. (samples with thickness of 8 mm, tested under a crosshead speed 5 mm/min, aged 3 months at three temperatures 25, 60 and 90 °C in distilled water).

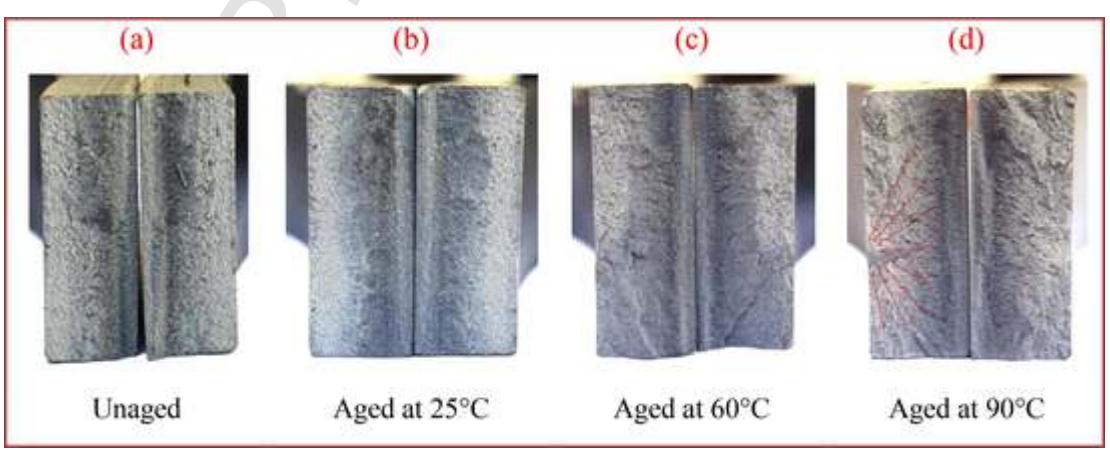

Fig. 14. Images of fracture surfaces of unaged and aged C-shaped PVC samples tested under CTPB.

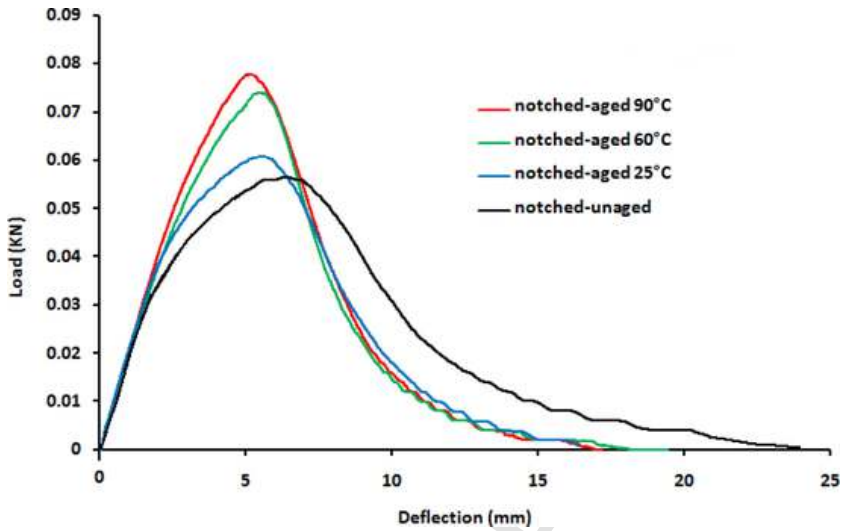

Fig. 15. Load-Deflection curves of virgin samples and hydrothermally aged pipe samples containing notch. (samples with thickness of 8 mm, tested under a crosshead speed 5 mm/min, aged at 3 months at three temperature 25, 60 and 90 °C in distilled water).

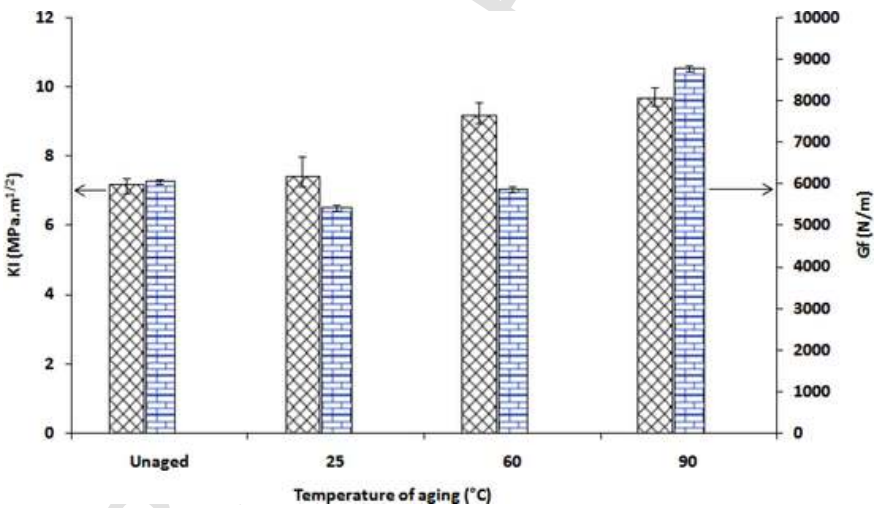

Fig. 16. Evolution of stress intensity factors (KI) and fracture energy (Gf) versus the temperature of aging, for initially notched samples. The unaged sample is considered as a reference.

Fig. 3a and b illustrate the boundary conditions and the adopted mesh of both model concave side up and down which have been designed as three dimensions (3D) model. Fig. 3-c illustrates the notched PVC model which has been considered as two dimensions (2D) in order to save calculation time since a damage model will be used in this case. Regarding the model with the concave side up and down (Fig. 3-a and b) both punch and supports have been modeled as analytical rigid body and the PVC pipe has been modeled as deformable with an elasto-plastic mechanical behavior determined by a tensile test mentioned in previous studies [22]. A velocity of V = 0.083 mm/s has been applied in the punch reference point (RP). The supports which radius is R = 5 mm have been constrained. A surface to surface contact interaction has been used between the rigid body and the pipe sample. A linear hexahedral C3D8R (A 8-node linear brick, reduced integration, hourglass control) elements as illustrated in Fig. 3. The number of the elements and nodes for the concave side up and down model are (7920 nodes, 5260 elements) and (8040 nodes, 5340 elements), respectively. In order to obtain accurate results a mesh refinement has been used in the contact between (supports, punch) and the pipe sample. Concerning the notched model presented in Fig. 3-c, it worth to note that the elasto-plastic behaviour was coupled with Extended Finite Element Method (XFEM) in order to simulate the damage taken place in the notched area. Table 2 presents the adopted parameters. The maximum principal stress was determined from the stress strain curve obtained by a tensile test. The fracture energy was calculated from the experimental flexural test conducted in the present study. The crack initiation is characterized by a width of l = 0.4 mm and a depth of a_0 = 1,2,3 and 4 mm. It is important to note that a quadratic element with reduced integration CPE4R has been used during simulation. The total numbers of nodes and elements is 1865 and 1613, respectively. The friction coefficient on the contact surfaces meets Coulomb friction law and it is determined with a tribological test, using pin-on-disk apparatus [10].

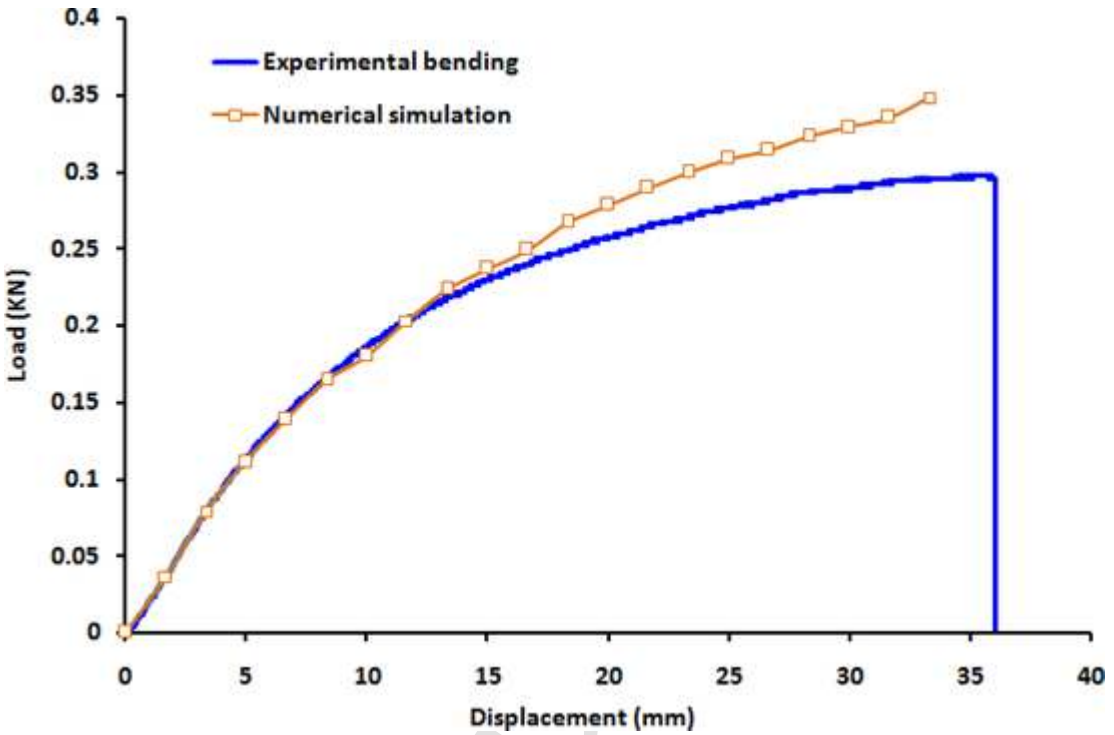

Fig. 17. Load displacement curve of the three-point bending test (Model 1).

3. Results and discussion

In this section, the experimental results obtained from curved three point bending (CTPB) tests are analyzed. Therefore, numerical results are compared with experimental data obtained from flexure tests.

3.1. Effect of crosshead rate on flexure response

Since most polymers exhibit viscoelastic behavior, their mechanical properties are time-dependent, the test results may be influenced by crosshead rate. In this study the bending tests were carried out at crosshead rates of 0.5, 5, 50, 250 and 500 mm/ min.

Fig. 4 shows representative flexural stress–flexural strain curves from curved three point bending tests of the pipe samples under the mentioned values of crosshead rate.

It is to note that all flexural properties (flexural strength (σ_f), flexural modulus (E_f) and strain to failure (ε_f)) were extracted from the obtained curves (Fig. 4) and then summarized in Table 3.

As can be observed in Fig. 4, all flexural stress–strain curves show similar trends. Three stages can be distinguished. The common pattern consists of an initial linear elastic deformation (stage 1), subsequent nonlinear response (stage 2), and a final failure where the stress drops suddenly (stage 3). Whatever, the retained value of crosshead speed, the pipe samples display ductile behaviour.

On the other hand, when varying the value of crosshead rate, the flexural properties change. This indicates the viscoelastic character of pipe material. In addition, the mechanical properties increase when the crosshead rate increases. In addition, when looking at the area under the load - deflection curves, we found that this area increases with the cross-head rate (from 0.5 to 500 mm/min). Such area is known to be proportional to the energy absorption capacity or the fracture energy, according to Kozłowski et al. [24].

Thus, the tendency for energy to increase as the crosshead rate is increased, may be ascribed to the failure mode of the pipe material since at a higher test speed, material yielding increases, thus more energy is expended during fracture process. These findings are in good agreement with these obtained by Okoli [25] in the case of fibre reinforced composites. Recently, Cui et al., [26] have also observed a significant improvement of the energy absorption capacity at the higher strain rates (from low to high) in their study regarding the tensile behaviour of thermoplastic composites. Also, similar trend was reported by Jacob et al., [27] regarding the evolution of flexural strength when increasing the loading rate or strain rate in the case of polymer composite materials. Similarly, Sims [28] has shown in his investigation on polyester/glass fibers composites, that the flexural strength increases with increasing loading rate form 10^{-6} to 10^{-1} mm/min.

On the other hand, Fig. 5 shows typical images of fracture surfaces from CTPB tests. It is possible to identify the differences in fracture mechanisms. The fracture becomes more and more brittle by increasing the speed rate. Similar observations were found by El-Bagory et al. [29] when studying the crack growth in PVC pipes.

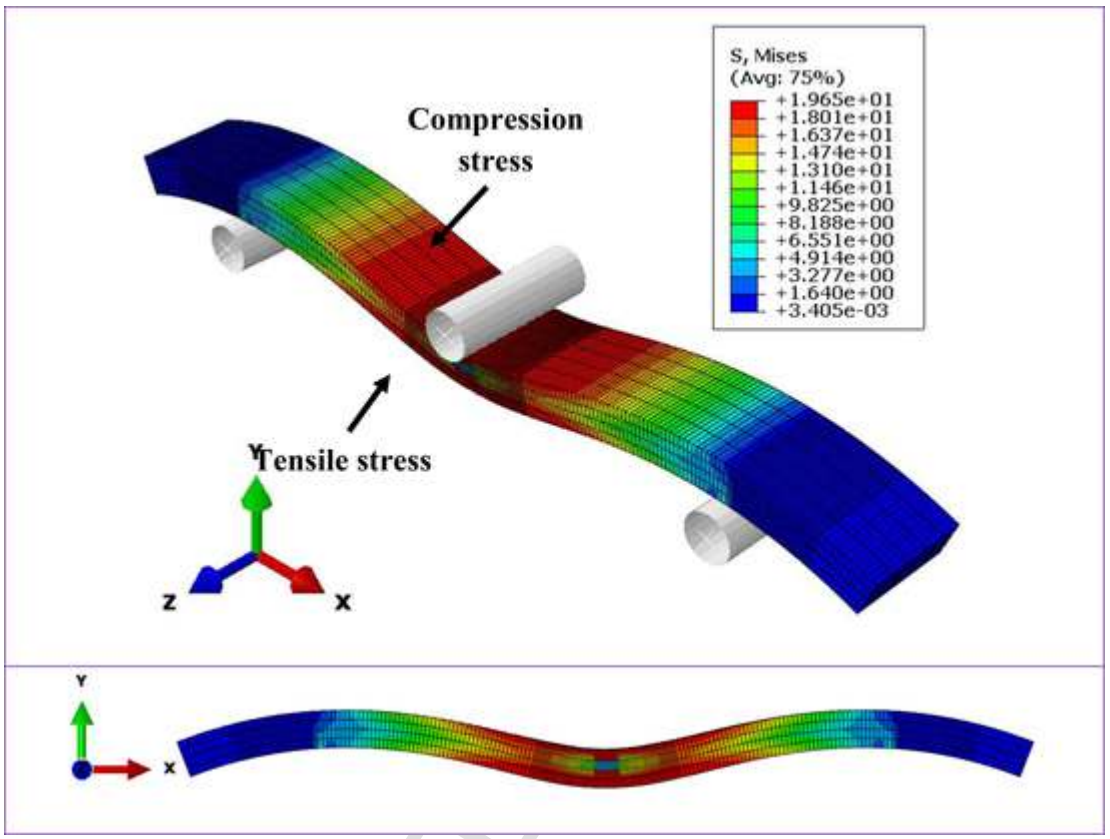

Fig. 18. Von Mises stress distribution throughout the PVC pipe (concave side down).

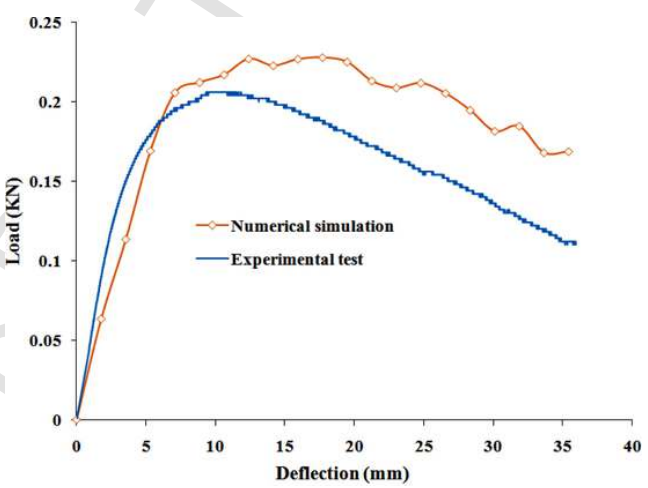

Fig. 19. Load -deflection curve of the three-point bending test (Model 2).

3.2. Effect of the 3-point bending configuration

Since the pipe material, in service, can be subjected to internal pressure as well as to external pressure, the following configurations were considered in our study, as shown in Fig. 6. The first configuration (Fig. 6-a) represents the case when the mechanical loading takes place on the external side of the pipe material. The second one (Fig. 6-b) simulates the case when the mechanical constraint takes place on the internal side of the pipe material (radial direction).

The average plots in Fig. 7 exhibit the typical results obtained from curved three point bending tests, using different configurations.

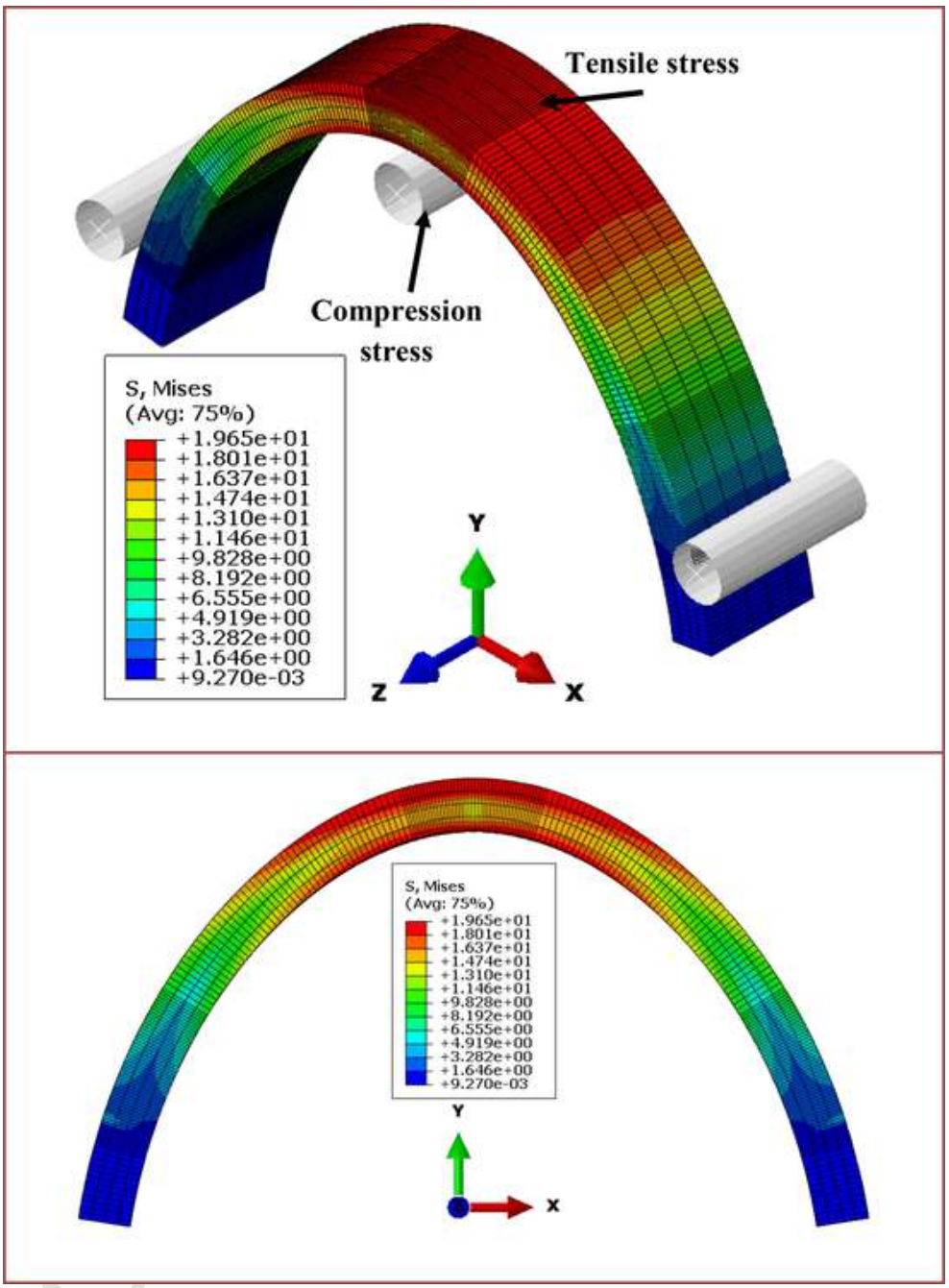

Fig. 20. Von Mises stress distribution throughout the PVC pipe (Model 2).

As seen in Fig. 7, when the direction of applied force is reversed, the mechanical response of the pipe material changes. Different behaviors are observed under internal or external mechanical loading even if there is the same level of pressure. The difference in the behavior seems to be the different structural configuration of the samples, samples and geometrical restraints.

The first difference consists in the flexural stiffness which represents the linear part of the load–deflection curve [30]. It was estimated as the curve-slope ($\Delta F/\Delta\delta$) between 10 and 50% of the ultimate load which represent the range before the "first crack initiation" and the "beginning of the elastic–plastic stage", according to Refs [31,32].

The plotted curves display that when the pipe sample is tested in configuration "concave side down ", its flexural stiffness was largely greater than in configuration "concave side up ".

Also, in order to confirm this hypothesis and quantify the sample performance in each case, we have estimated the fracture energy, G_F, using the following equation:

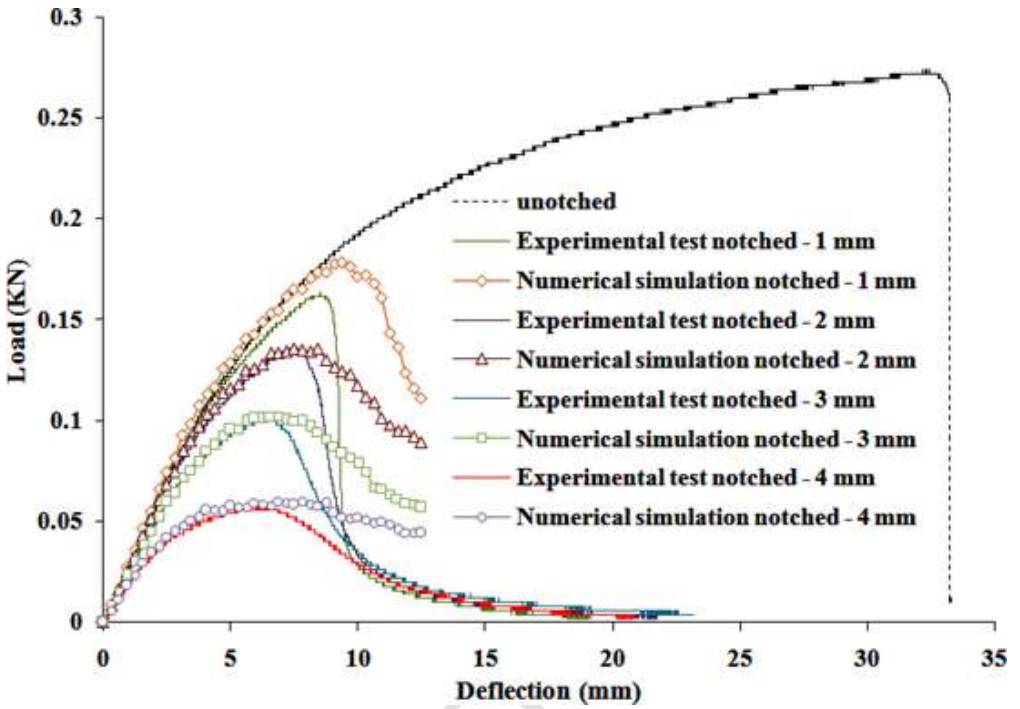

Fig. 21. Load-deflection curve of the three-point bending test (Model 3).

$$G_F = \frac{(A + (m * g * \delta))}{((\mathrm{h} - a)(* W)} \tag{4}$$

Where:
a: the notch depth (m).
A: the area of the complete load–deflection curve, (N/m).
W: the width of the sample (m).
h: thickness of the sample (m).
m: the weight of the sample (Kg).
g: the acceleration due to gravity (m/s^2).
δ: the deformation at the final failure of the sample (m).

Also, from Fig. 7, the values of fracture energy, G_F, were found about 49 253 N/m and 42 416 N/m for "concave side down" and "concave side up" configurations, respectively. The fracture energy, G_F, increases by 14% where curved samples were tested in configuration "concave side down ". This confirms again the obtained trend in terms of flexural stiffness.

In addition, in the configuration of " concave side down ", peak pipe loads occurs at smaller displacements. This means that the resistance of pipe material reaches rapidly its maximum point (the material yielding). Then, it decreases progressively until reaching the failure point. Whereas, in the configuration of " concave side up ", the flexural response of pipe material is characterized by a first linear deformation, non-linear deformation and brutal failure. In this case, peak loads occurs at very larger deflections. The pipe material seems to be more ductile, and a gain of ductility of 12% was observed. This means that internal pressure is more dangerous than external pressure for the lifetime of pipe material.

3.3. Effect of notch and notch depth

In this section, we look firstly to predict the failure load of samples containing sharp V-notches. Such load value could be helpful to estimate the average stress or the external pressure responsible for pipe damage. After that, we will examine the effect of notch depth on flexural response of tested samples. Here, all bending tests were carried out on pipe samples (of 8 mm of thickness) at crosshead rate of 5 mm/ min (Fig. 8). For notched samples, four values of notch depths "a" are tested: a = 1 mm, 2 mm, 3 mm and 4 mm which means $a/h = 0.125$; 0.25; 0.375 and 0.5 where "h" represents the sample thickness.

In order to conduct a comparative study between all the tested samples, we have focused on two parameters: the stress intensity factor $\boldsymbol{K_I}$ and the fracture energy $\boldsymbol{G_f}$. These parameters can be extracted from Load-Deflection curves (Fig. 8). According to Lee et al., [33], the stress intensity factor K_I ($MPa.m^{1/2}$) is calculated using the following equations and according Fig. 9.

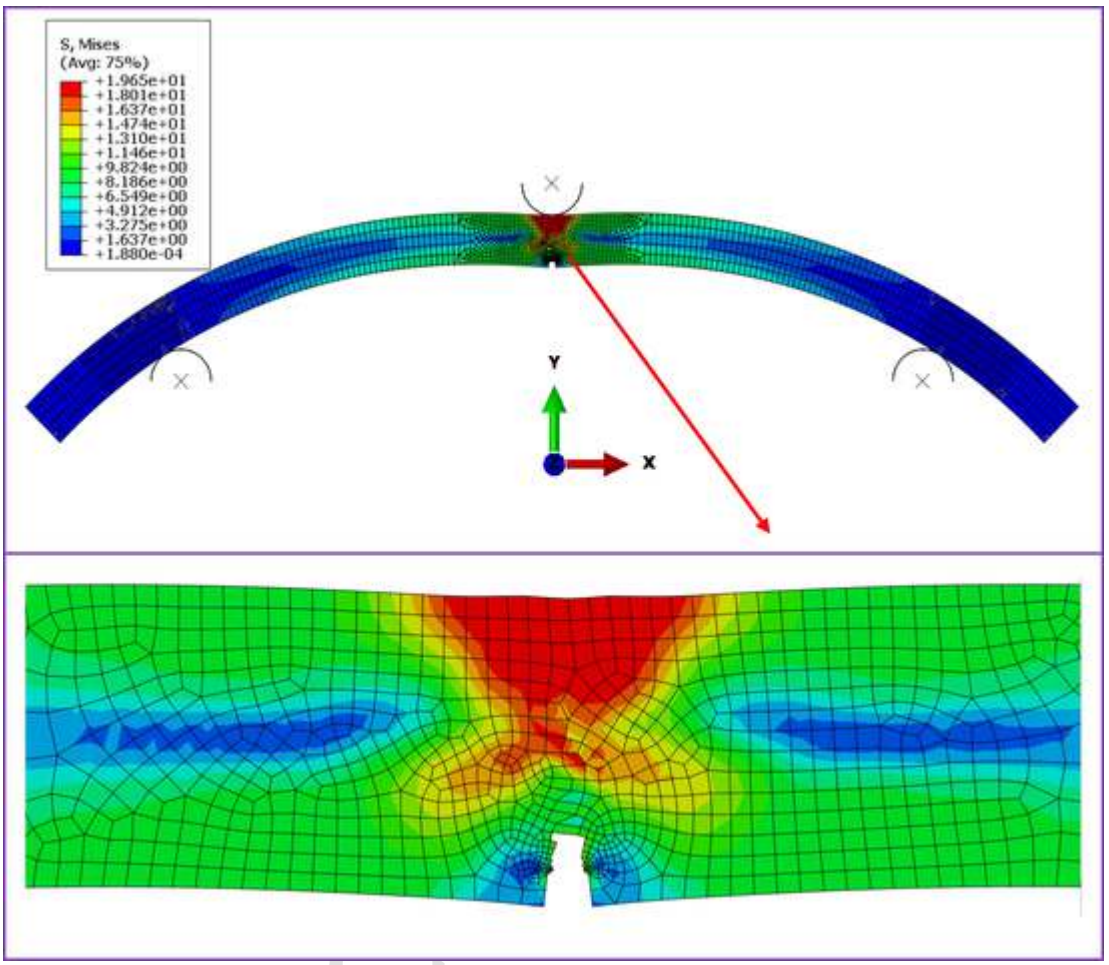

Fig. 22. Von Mises stress distribution throughout the PVC notched pipe –1 mm (Model 3).

$$K_I = \frac{P\tan\theta}{\sqrt{R_e B}} f\left(\frac{a}{h}\right), \tag{5}$$

$$f\left(\frac{a}{h}\right) = \sqrt{R'}\left[\frac{3R_i}{R_e}\left(1-\frac{R_i}{R_e}\right)^{-3/2} Y_1(R') + \frac{1}{2}\left(1-\frac{R_i}{R_e}\right)^{-1/2} Y_2(R')\right] \tag{6}$$

$$R' = \frac{R/R_e - R_i/R_e}{1 - R_i/R_e} = \frac{a}{h}$$

$$Y_1(R') = 1.39 - 3.07\frac{a}{h} + 14.53\left(\frac{a}{h}\right)^2 - 25.11\left(\frac{a}{h}\right)^3 + 25.8\left(\frac{a}{h}\right)^4$$

$$Y_2(R') = 1.99 - 0.41\frac{a}{h} + 18.07\left(\frac{a}{h}\right)^2 - 38.48\left(\frac{a}{h}\right)^3 + 53.85\left(\frac{a}{h}\right)^4$$

Similarly, the fracture energy is estimated according to the following formula, [32]:

$$\mathrm{Gf} = \frac{Total\ \ dissipated\ \ work}{Sectional\ \ dimensions} \tag{7}$$

where the total dissipated work is the area under the curve and the sectional dimensions ($w \times h$) represent the Euclidian fracture surface.

Fig. 10 plots the variation of stress intensity factors (KI) and Fracture energy (Gf) versus the ratio (notch depth / sample thickness: a/h).

Fig. 10 shows clearly that the energy involved in the failure of pipe samples as estimated from the area under the load–deflection curves decreases enormously for notched samples compared to unnotched samples. This can be explained by the fact that unnotched pipe samples require greater energy to be deformed compared to samples containing initial crack.

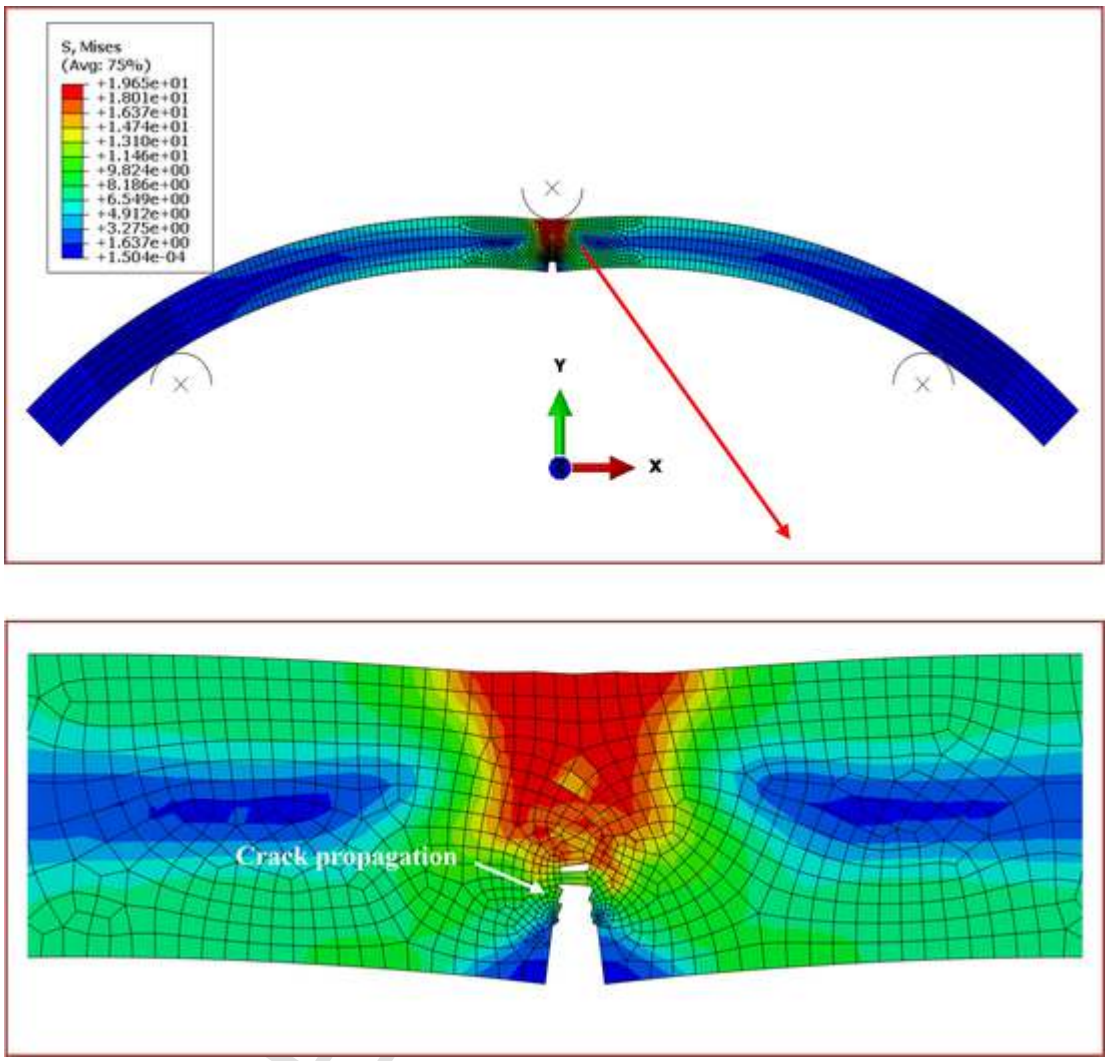

Fig. 23. Von Mises stress distribution throughout the PVC notched pipe −2 mm (Model 3).

Moreover, the fracture energy appears to decrease when the depth of initial crack increases.

On the other hand, the sequences of notch propagation of the notched samples during the flexural tests are illustrated in Fig. 11. It can be observed that a single critical crack was initiated from the notched section and propagated to upper part of the sample as the load increases. It can be also seen that even after reaching the flexural strength, and the load starts to decrease, the crack continues progressively to open until the complete rupture or final fracture of tested sample.

In terms of fracture surfaces, Fig. 12 shows typical images of notched samples with a depth from 1 to 4 mm from CTPB tests. It is clear that as the depth of the notch is increased, the fracture becomes more and more ductile. This is can be explained by the disappearance of the slight river lines showed in Fig. 12-(a) and replaced by material tear-off zones in Fig. 12-(b),(c) and (d). The same ductile tearing was identified by Rodolfo et al. [34] when using various fracture mechanics methodologies for the characterization of PVC pipes.

3.4. *Effect of hydrothermal aging*

Given that polymeric pipes can be exposed, in service, to severe weathering conditions (temperature, humidity), we look here to examine firstly if the retained hydrothermal aging affects the flexure response of pipe material. After that, it will be important to know how the pipe material behaves under the combined effect of aging and notch.

Fig. 13 displays the average plots of load–deflection curves for virgin and hydrothermally aged (3 months at three temperature 25, 60 and 90 °C in distilled water) pipe samples. Here, three stages can be observed, a linear elastic deformation, nonlinear response and a final failure. Also, Fig. 13 clearly exhibits that *i)* all aged samples have higher (max) tensile stress (they break at higher stresses) respect to the unaged one and *ii)* the failures of the aged samples, at 25 and 60 °C, occurred earlier than the unaged one.

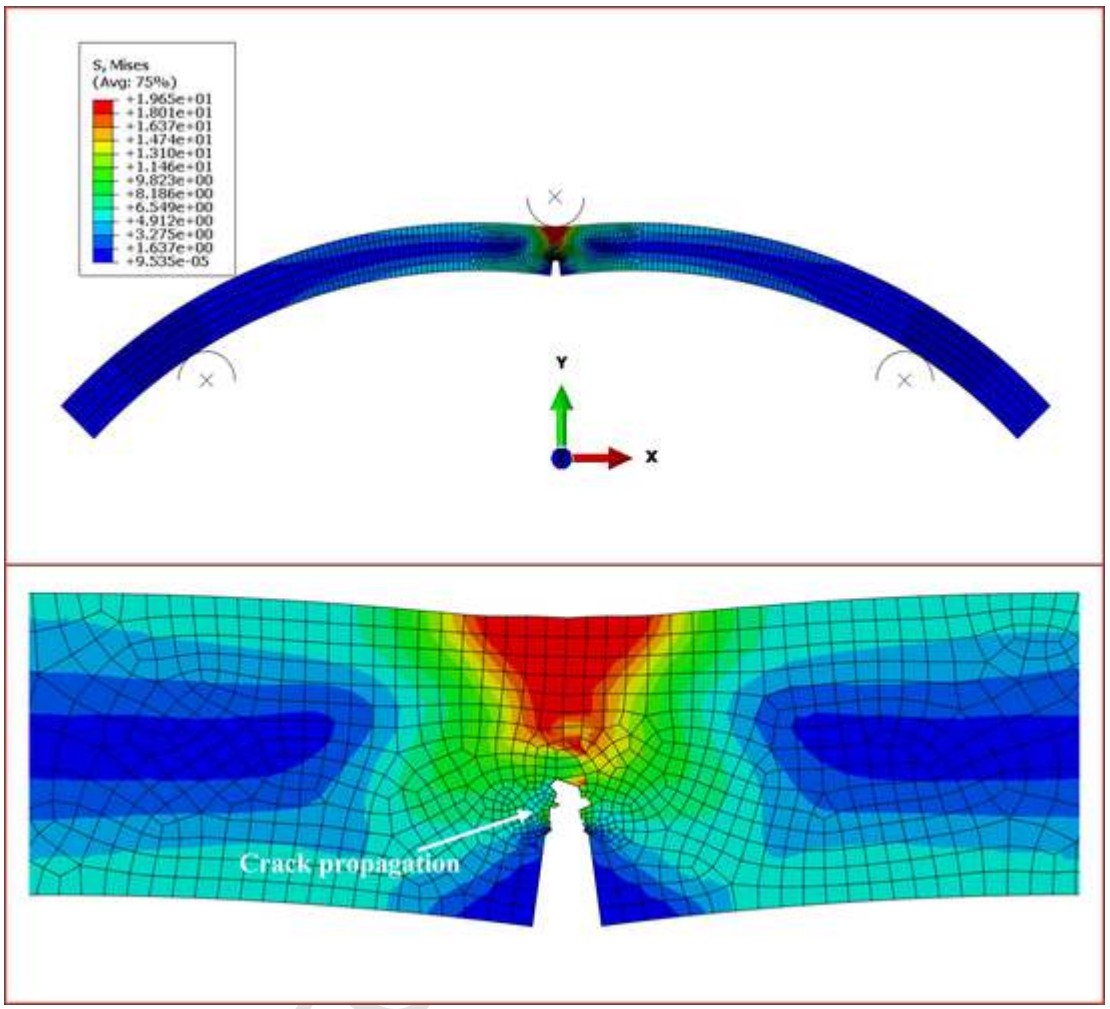

Fig. 24. Von Mises stress distribution throughout the PVC notched pipe −3 mm (Model 3).

In addition, as shown in Fig. 13, the area of the load–deflection curve of the 25 ˚C aged sample is less than the one of unaged sample. This can be explained by the fact that the material becomes more brittle with the aging.

However, as obviously observed in Fig. 13, the area under the load–deflection curve of the 90 ˚C aged sample is still larger than the others. This clearly means an higher absorbed energy before fracture. Also, the area of the load–deflection curve of the 90 ˚C aged sample is larger than the one of unaged sample. This behaviour can equally be explained, firstly by the phenomenon of migration of plasticizers at higher temperatures which improves toughness (the sample is tougher). In fact, plasticizers leave the place to the particles of $CaCo_3$ and voids, and like that the structure loses its softness as previously explained in Ref. [10]. The increase of the density of $CaCo_3$ in the material structure, leads to an increase in stiffness.

Fig. 14 presents the effect of aging on the fracture surface of pipe samples. The aging has a positive effect in term of stiffness but it accelerates the time of fracture. The 25 and 60 ˚C aged samples becomes more brittle. The fracture surface of the 90 ˚C aged sample is characterized by the appearance of the slight river lines pointing to the same zone (Fig. 14-(d)).

On the other hand, Fig. 15 displays the load–deflection curves of both virgin samples and hydrothermally aged pipe samples containing notch (depth of 4 mm). The obtained data, which are extracted from Fig. 15, are summarized in Fig. 16. Here, it is obvious that both the stress intensity factors *(KI)* and Fracture energy *(Gf)* increase with the aging temperature. This indicates greater impacts of hygrothermal aging on these characteristics. This finding agree well with those obtained by Omranian et al., [35] in their study about the fracture properties of mixtures subjected to different ageing conditions.

As shown in Fig. 16, the stress intensity factor and fracture energy increased with the aging temperature. This can be explained by the fact that the temperature accelerates the migration of plasticizers as previously described in Ref. [36].The resulting porosity and voids can serve to impede, arrest, or deflect the crack as found in Ref. [37]. Thereby, improving the extrinsic toughness of the material.

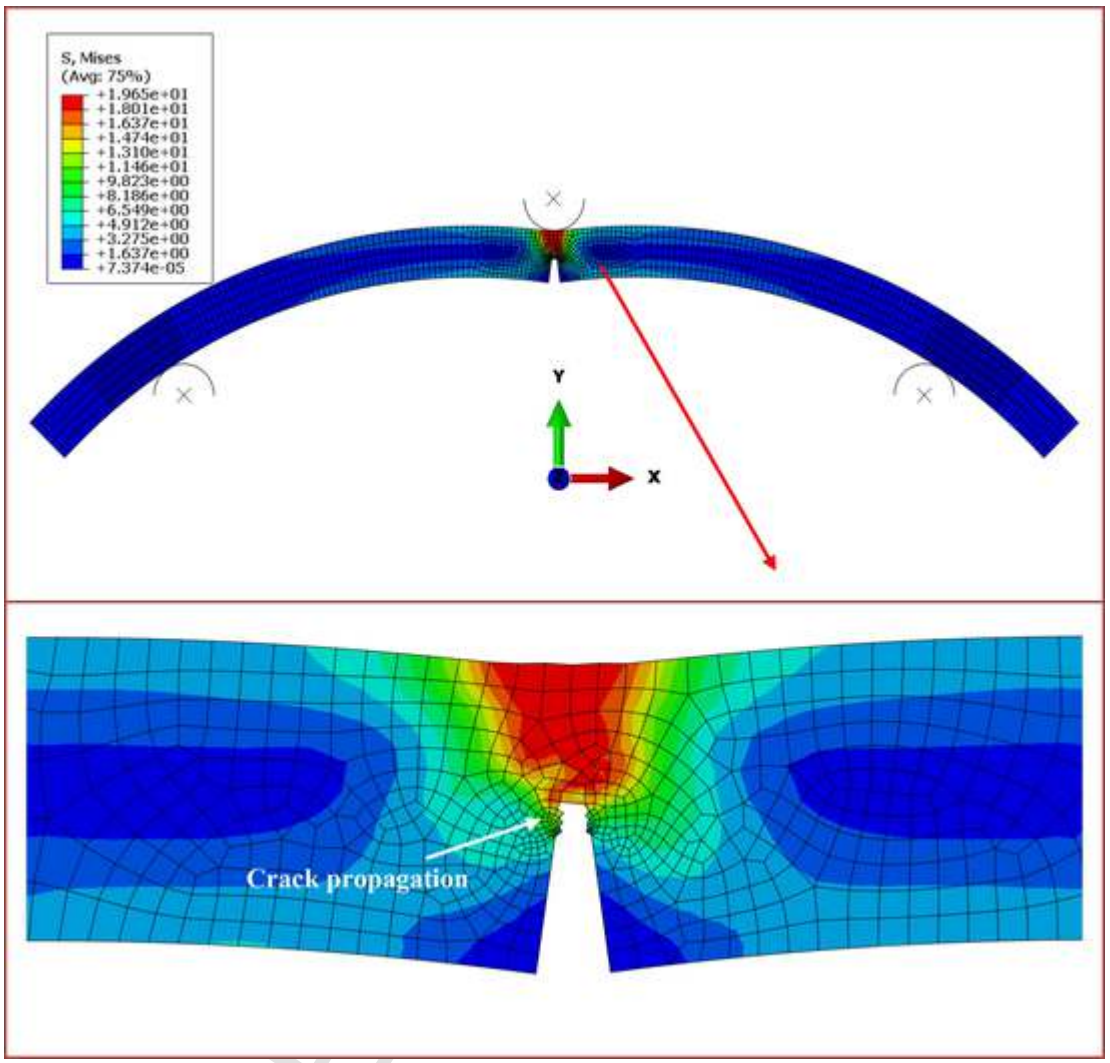

Fig. 25. Von Mises stress distribution throughout the PVC notched pipe –4 mm (Model 3).

3.5. Numerical modeling results

In the present section, three-point bending test was conducted on the pipe sample for the model concave side down. Fig. 17 illustrates a comparison between the load–deflection curve of the numerical and experimental test. A good agreement was found between the experimental and the numerical results. The experimental curve exhibits an elasto-plastic behavior and reach a maximum of F = 304 N. The numerical curve follows perfectly the experimental ones. It is important to note that the discrepancy found between the experimental curves can be related to the experimental error when cutting samples which can affect relatively the evolution of the load–deflection curve as mentioned in similar research [38].

Fig. 18 illustrates the Von Mises stress distribution throughout the PVC Pipe of the model (concave side down). It can be observed a compression and a tensile stress on the top and the bottom surface of the PVC pipe. The maximum stress reaches 19.6 MPa which presents the maximum tensile strength mentioned in previous research [20] indicating the damage of the PVC pipe in the middle area. Unlike the middle area throughout the thickness, the stress which has been recorded in the PVC pipe is equal to 1.63 MPa which correspond to (medium fiber).

As seen in Fig. 19 a good agreement was found between the experimental and the numerical results. The experimental curve exhibits an elasto-plastic behavior and reaches a maximum of F = 304 N. The numerical curve follows perfectly the experimental displacement value of D = 16.65 mm. The small deviation may be attributed to the experiment conditions. The ratios of the FE model to the experimental deflections (or load) at the load peak range from 0.9 to 1.0, indicating a good correlation with the experimental results.

Fig. 19 illustrates the load–deflection curve of the model (Concave side up). It can be observed a linear evolution at the beginning. The discrepancy between the numerical and the experimental curve is more important than the first model. Then, the

load–deflection curve exhibits a plastic deformation to reach a maximum load F = 0.22 kN. Finally, it can be observed a decreasing of the recorded load similar to the experimental one. Fig. 20 presents the Von Mises stress distribution throughout the concave side up model. It can be detected a compression and a tensile stress concentrated in the concave and convex side, respectively. The ratios of the FE model to the experimental deflections (or load) at the load peak range from 0.9 to 1.0, reflecting a good relationship with the experimental results.

In the present section, numerical simulations were conducted for the notched model. An XFEM damage technique has been used in order to reproduce the crack propagation in every model. The maximum principal stress (Maxps) damage criteria has been used during simulation. It is important to note that the fracture energy has been introduced for the damage evolution based on the experimental test. Four notches are analyzed, 1 mm, 2 mm, 3 mm and 4 mm. Fig. 21 displays a comparison between the experimental and the numerical curve of unnotched and the notched model. A good agreement has been found between curves until the maximum load is reached, then a small gap can be observed in the damage part of the curves. The initial behavior observed in all curves until crack nucleates is almost elasto-plastic due to the materials modeling of the PVC pipe. The crack propagation throughout the thickness of the pipe generates a decreasing in the load until reaching the total fracture of the Pipe. The effect of the notch length can be clearly seen in the load–deflection curve. As the notch length increases the maximum recorded load decreases as discussed in the experimental section.

The Von Mises stress distribution throughout the cross section of the model with notch length equal to 1 mm is presented in Fig. 22. It can be seen that the maximum stress concentration is localized in front of the notch. The notch effect in the stress distribution throughout the thickness of the PVC pipe can be observed clearly when comparing with unnotched model. Furthermore, the crack is propagated perpendicular to the solicited surface. Figs. 23, 24 and 25 illustrate the Von Mises stress distribution for crack length equal to a = 2 mm, a = 3 mm, a = 4 mm, respectively. Similar stress distribution can be observed. It can be remarked that the stress concentration area decreases with increasing the crack length.

Conclusion

In the present study, experimental and numerical studies of three-point bending test for PVC pipe have been conducted. The obtained results and the correlation between the experimental and the numerical approach permit to deduce that for all configurations and parameters retained in flexural tests, load–deflection or stress–strain responses, of pipe materials, showed typical features of thermoplastics, characterized by an elastic regime, followed by a nonlinear deformation up to yield peak, and subsequent brittle failure. The flexural response of pipe materials largely depend on the test factors: the direction of the applied mechanical loading (internal or external pressure), with and without initial notches, notch depths, hydrothermal aging. Both of the stress intensity factors *(KI)* and Fracture energy *(Gf)* increase with the aging temperature. Also, the fracture energy decreases when the depth of initial crack increases. The stress–strain behaviour of material pipe, in most cases, fits well with the established FE model that can be used in the design of pipe structures.

Finally, the introduction of a failure criteria for the numerical simulations may help to well model the behavior of polymeric materials for a large range of strain rate, and to distinguish brittle and ductile failure for tested material. This improvement needs a further study.

Declaration of Competing Interest

The authors declare that they have no known competing financial interests or personal relationships that could have appeared to influence the work reported in this paper.

Acknowledgements

The authors gratefully acknowledge Tuyauplast company (Gafsa, Tunisia) for providing the polymeric pipes used in this research.

References

[1] F.M. Peres, C.G. Schön, An alternative approach to the evaluation of the slow crack growth resistance of polyethylene resins used for water pipe extrusion, J. Polym. Res. 14 (3) (2007) 181–189.
[2] N. Kiass, R. Khelif, L. Boulanouar, K. Chaoui, Experimental approach to mechanical property variability through a high-density polyethylene gas pipe wall, J. Appl. Polym. Sci. 97 (1) (2005) 272–281.
[3] H. Benyahia, M. Tarfaoui, A. El Moumen, D. Ouinas, O.H. Hassoon, Mechanical properties of offshoring polymer composite pipes at various temperatures, Compos. B Eng. 152 (2018) 231–240.
[4] F.J. McGarry, J.F. Mandell, L. Hsueh-Lee, Brittle fracture in PVC pipe material. Journal of Polymer Science: Polymer Symposia (Vol. 72, No. 1, pp. 83-110). New York: Wiley Subscription Services, Inc., A Wiley Company, , 1985.
[5] R. Sikora, The effect of heating of PVC pipes on selected mechanical properties of pipe bells, Polimery 43 (1998) 384–389.
[6] J. Yu, L. Sun, C. Ma, Y. Qiao, H. Yao, Thermal degradation of PVC: a review, Waste Manage. 48 (2016) 300–314.
[7] N. Guermazi, N. Haddar, K. Elleuch, H.F. Ayedi, Effect of filler addition and weathering conditions on the performance of PVC/CaCO3 composites, Polym. Compos. 37 (7) (2016) 2171–2183.
[8] H. Stichnothea, A. Azapagic, Life cycle assessment of recycling PVC window frames resources, Conserv. Recycl. 71 (2013) 40–47.
[9] F.C. Amorim, J.F.B. Souza, H.S. Costa Mattos, J.M.L. Reis, Temperature effect on the tensile properties of unplasticized polyvinyl chloride, SPE Polym. 3 (2) (2022) 99–104.
[10] H. Jemii, A. Boubakri, A. Bahri, D. Hammiche, K. Elleuch, N. Guermazi, Tribological behavior of virgin and aged polymeric pipes under dry sliding conditions against steel, Tribol. Int. 106727 (2020).

[11] M. Balkaya, I.D. Moore, A. Saglamer, Study of non-uniform bedding support under continuous PVC water distribution pipes, Tunn. Undergr. Space Technol. 35 (2013) 99–108.
[12] A. Sotayoa, S. Greena, G. Turvey, Experimental investigation and Finite Element (FE) analysis of the load deformation response of PVC fencing structures, Structures 19 (2019) 424–435.
[13] M. Fakharifar, G. Chen, FRP-confined concrete filled PVC tubes: A new design concept for ductile column in seismic regions, Constr. Build. Mater. 130 (15) (2017) 1–10.
[14] J. Kang, Y. Jung, Y. Ahn, Cover requirements of thermoplastic pipes used under highways, Compos.: Part B 55 (2013) 184–192.
[15] F.G. Al-Abtah, E. Mahdi, S. Gowid, The use of composite to eliminate the effect of welding on the bending behavior of metallic pipes, Compos. Struct. 235 (2020) 111793.
[16] S.E. Firouzsalari, D. Dizhur, K. Jayaraman, N. Chouw, J.M. Ingham, Flax fabric-reinforced epoxy pipes subjected to lateral compression, Compos. Struct. 244 (2020) 112307.
[17] M. Babiak, M. Gaff, A. Sikora, Š. Hysek, Modulus of elasticity in three-and four-point bending of wood, Compos. Struct. 204 (2018) 454–465.
[18] J.F. Mandell, A.Y. Darwish, F.J. McGarry, Time and temperature effects on the fracture toughness of rigid poly (vinylchloride) pipe materials, Polym. Eng. Sci. 22 (13) (1982) 826–831.
[19] C. Aldea, S. Marikunte, S.P. Shah, Extruded fiber reinforced cement pressure pipe, Adv. Cem. Based Mater. 8 (2) (1998) 47–55.
[20] H. Jemii, A. Bahri, A. Boubakri, D. Hammiche, K. Elleuch, N. Guermazi, On the mechanical behaviour of industrial PVC pipes under pressure loading: experimental and numerical studies, J. Polym. Res. 27 (8) (2020) 1–13.
[21] N. Guermazi, A.B. Tarjem, I. Ksouri, H.F. Ayedi, On the durability of FRP composites for aircraft structures in hygrothermal conditioning, Compos. B Eng. 85 (2016) 294–304.
[22] H. Jemii, D. Hammiche, A. Boubakri, N. Haddar, N. Guermazi, Mechanical, thermal and physico-chemical behavior of virgin and hydrothermally aged polymeric pipes, J. Thermoplast. Compos. Mater. 892705720962167 (2020).
[23] J.B. Wachtman, Mechanical properties of porous ceramics, Mech. Propert. Ceram. (1996) 409–412.
[24] M. Kozłowski, M. Kadela, A. Kukiełka, Fracture energy of foamed concrete based on three-point bending test on notched beams, Procedia Eng. 108 (2015) 349–354.
[25] O.I. Okoli, The effects of strain rate and failure modes on the failure energy of fibre reinforced composites, Compos. Struct. 54 (2–3) (2001) 299–303.
[26] J. Cui, S. Wang, S. Wang, G. Li, P. Wang, C. Liang, The effects of strain rates on mechanical properties and failure behavior of long glass fiber reinforced thermoplastic composites, Polymers 11 (12) (2019) 2019.
[27] G.C. Jacob, J.M. Starbuck, J.F. Fellers, S. Simunovic, R.G. Boeman, Strain rate effects on the mechanical properties of polymer composite materials, J. Appl. Polym. Sci. 94 (1) (2004) 296–301.
[28] G.D. Sims, In Proceedings of the 6th International Conference on Composite Materials and 2nd European Conference on Composite Materials, Imperial College, London, 1988, Vol. 3, pp.3.494–3.507.
[29] T.M. El-Bagory, M.Y. Younan, Crack growth behavior of pipes made from polyvinyl chloride pipe material, J. Pressure Vessel Technol. 139 (1) (2017).
[30] S.I. Mohammed, K.B. Najim, Mechanical strength, flexural behavior and fracture energy of Recycled Concrete Aggregate self-compacting concrete, In Structures 23 (2020) 34–43.
[31] P. Zhang, Y.N. Zhao, Q.F. Li, P. Wang, T.H. Zhang, Flexural toughness of steel fiber reinforced high performance concrete containing nano-SiO2 and fly ash, The Scientific World J., 2014.
[32] K.B. Najim, A. Saeb, Z. Al-Azzawi, Structural behaviour and fracture energy of recycled steel fibre self-compacting reinforced concrete beams, J. Build. Eng. 17 (2018) 174–182.
[33] G.S. Lee, M.M. Epstein, Fracture surface features of polyethylene pipe samples, Polym. Eng. Sci. 22 (9) (1982) 549–555.
[34] Rodolfo Jr, Antonio, Application of fracture mechanics for the characterization of PVC pipes. I. Evaluation of the applicability of the EWF technique in specimens produced directly from pipes, J. Vinyl Additive Technol. 2020
[35] S.R. Omranian, M.O. Hamzah, T.S. Yee, M.R. Mohd Hasan, Effects of short-term ageing scenarios on asphalt mixtures' fracture properties using imaging technique and response surface method, Int. J. Pavement Eng. 21 (11) (2020) 1374–1392.
[36] H. Jemii, A. Bahri, R. Takatak, D. Hammiche, N. Guermazi, Flexural behavior and fracture characteristics of polymeric pipes under curved three-point bending (CTPB) tests. In: Bouraoui T. et al. (eds) Advances in Mechanical Engineering and Mechanics II. CoTuMe 2021. Lecture Notes in Mechanical Engineering. Springer, Cham, 2022.
[37] K.M. Conway, C. Kunka, B.C. White, G.J. Pataky, B.L. Boyce, Increasing fracture toughness via architected porosity, Mater. Des. 205 (2021) 109696.
[38] A. Bahri, N. Guermazi, M. Bargui, K. Elleuch, Estimation of the elastic modulus of the alumina coated AA1050 aluminum: modeling and experiments, Mater. Sci. Eng., A 670 (2016) 188–195.